Research on Underwater Noise Features Based on Spectrum Analysis and Welch Algorithm

Hui Zhou[1], Biyuan Yao[1,2], Kun Ye[3], Guiqing Li[2], Jin Guo[3]

[1] School of Computer Science and Cyberspace Security, Hainan University, China
[2] School of Computer Science and Engineering, South China University of Technology, China
[3] School of Science, Hainan University, China
zhouhui@hainanu.edu.cn, yaobiyuanyy@163.com, yekun_eric@163.com, ligq@scut.edu.cn, guojinecho@163.com

Abstract

To explore the characteristics of underwater noise, we analyze the power spectrum and frequency of underwater noise with the sequence diagram, the period diagram, the density diagram and improved welch algorithm according to the 5-day noise data by root mean square. The results show that, first of all, spectrum analysis and welch algorithm simplify the calculation process and adapt to the impulsiveness and randomness of noise. Secondly, adopting different window functions in welch power spectrum estimation improves the spectral resolution of underwater noise prediction, which is insensitive to noise. Thirdly, in the spectrum analysis, the accuracy of experimental results from welch algorithm obviously outperforms sequence diagram, periodic diagram and density diagram. Compared with periodic diagram and density diagram, the improved welch algorithm will obtain smoother power spectrum estimation, reducing the resolution and random error of noise frequency in the segmentation process. Finally, when the number of sites is greater than 10, our simulation results are more accurate than that with periodic diagram method.

Keywords: Underwater noise' features, Sequence diagram, Periodogram, Density graph, Welch algorithm

1 Introduction

The research on the characteristics of underwater noise is a hot topic in the marine field. It has a wide range of applications in military, seismic detection and other fields. In the military, the underwater noise generated by the radiation of ships, submarines and torpedoes destroys the concealment of ships, especially submarines, and provides search, detection and tracking information for the opponent's underwater acoustic detectors. Ship noise may cause some underwater weapons to explode. It leads to a decline in the military's combat effectiveness and its own security. At the same time, underwater acoustic guided weapons and acoustic fuze weapons attack each other based on underwater noise, so underwater noise characteristics are an important basis for the development of underwater weapons.

In seismic exploration, underwater noise measurement, as a marine acoustic remote sensing method, can be used to estimate relevant seismic environmental parameters. Monitoring underwater biological noise and man-made noise can also be used to study the physical mechanism and statistical features of underwater noise generation and propagation. Underwater noise is the background interference existing in the underwater acoustic channel, which interferes with sonar operation and limits the performance of sonar system. Data source: In 2016, the scientific research group conducted 5-day sea trials in Qiongzhou Strait, China. Nine sites are selected in the test, and different voltages are used to test underwater noise. The sample frequency is 50 Hz, and root mean square noise data of 9 sites in 5 days (Table 1).

Table 1. Root mean square noise data

Site	Noise				
	Day1	Day2	Day3	Day4	Day5
1	143.50	136.33	137.33	145.17	138.81
2	145.85	138.89	143.30	139.22	138.11
3	-	139.92	139.13	137.38	145.19
4	140.37	139.39	139.49	141.18	138.17
5	135.72	140.72	142.14	138.29	137.94
6	142.64	147.48	140.53	135.79	135.81
7	146.12	136.74	144.58	138.25	139.71
8	135.58	139.34	151.08	138.83	140.23
9	-	137.52	139.18	141.95	141.81

The **innovations** of the paper: (*i*) the use of spectrum analysis and welch algorithm to study the characteristics of underwater noise is more simple and faster in calculations, and can adapt to the impulse and randomness of noise. (*ii*) Choosing an appropriate windowing function $w(n)$ and adding it directly before the period diagram calculation. No matter which

*Corresponding Author: Guiqing Li; E-mail:ligq@scut.edu.cn
DOI: 10.3966/160792642021052203020

windowing function is added, spectrum estimation can be made non-negative. Welch power spectrum estimation algorithm directly predicts short signal underwater noise with low spectral resolution, and the signal is also prone to be interfered by noise, leading to inaccurate prediction, so short-term signals cannot be realized by this algorithm. We use different window functions to join welch power spectrum estimation algorithm, which can improve the spectral resolution of underwater noise prediction and is not susceptible to noise. When adding a window function, different window functions will have their own shortcomings, so we use four window functions to make up for their shortcomings. When segmenting, we overlap the segments with unequal distances, which will reduce the variance. Our results are consistent with the expected accuracy. (*iii*) By comparing the analysis results, it can be seen that the accuracy of the analysis results of welch algorithm is significantly better than the sequence diagram, the period diagram and density diagram in the spectrum analysis. The limitations of the paper: the sample frequency is 50, the sample time is 5 days, and the sample points are 7, 9, 9, 9 and 9, respectively. Therefore, it has a smaller amount of data and lower resolution.

The contents of this paper are organized as follows. We review previous studies which related to features of underwater noise in section 2. Section 3 is the basic theory. In section 4, the noisy characteristics are studied through the noise sequence diagram, periodic diagram, density diagram, and combined with the noise voltage intensity, frequency and amplitude of different sites. Section 5 is welch algorithm, which analyzes the underwater noisy characteristics through four different window functions of rectangular, hamming, Blackman and hanning. The conclusion is given in section 6.

2 Related Works

Aiming at the passive detection of the azimuth, frequency and line spectrum signal frequency radiated by underwater weak targets, Luo and Shen [1] proposed a space-frequency joint detection and tracking method based on the tracking-before-detection technology. This method has good performance of line spectrum detection at low signal-to-noise ratio, and can adapt to complex situations such as multi-target and multi-line spectrum signals. Merchant et al. [2] used the power spectral density to evaluate passive acoustic monitoring performance and the statistical distribution of underwater noise. This method is combined the average value and percentile of the spectrum as a standard integrated representation of the environmental noise spectrum. Qi et al. [3] used the combined algorithm of welch power spectrum estimation and median filter to extract the linear spectrum of the underwater vehicle radiated noise, and some dominant frequencies are determined. In view of the difficulty in determining the variation of noise law from the perspective of theory and experiment, Meng et al. [4] studied the random characteristics of ocean noise through statistical analysis methods such as mathematical expectation, variance, and power spectral density. Hovem et al. [5] analyzed underwater noise by Fourier transform, spectral analysis and time-frequency analysis, and made a conclusion that noise propagation is affected by the Lloyd's mirror effect. Underwater noise is composed of steady and transient signals. Liu [6] extracted underwater noisy characteristics by using short-time Fourier transform of the transient signal and Wigner distribution. It showed that the smooth Wigner distribution method can accurately extract the time-varying rule and influence spectrum range of ship underwater transient noise. Huang [7] used the frequency estimation algorithm of power spectrum and phase information to solve the frequency estimation of line spectrum signal. In this paper, it improves the discrete Fourier transform and the least square frequency estimation algorithm and proposes the frequency estimation algorithm of digital orthogonal transform. Shaameri et al. [8] used the power spectral density, autocorrelation function and non-Gaussian probability density function to analyze different real-time noise data. The results showed that the power of underwater noise decreases by increasing of the depth, since the distance from the surface is about 10dB. Yan et al. [9] obtained the power spectrum characteristics of ship radiated noise by welch power spectrum estimation method, and proposed a classification and recognition method of ship radiated noise based on depth self-code network. Cui et al. [10] analyzed the power spectral density and propagation characteristics of UWB pulses with different frequencies in different underwater distances by using welch spectral analysis method. Ju et al. [11] collected the underwater noise generated by four different types of riprap construction, and analyzed the sound pressure level and power spectral density of the acoustic signal. Yan and Zhang [12] used welch algorithm and median filtering joint algorithm to extract the line spectrum of underwater target radiated noise signal, and the two algorithms improve detection accuracy of the line spectrum.

3 Basic Theory

Spectrum analysis is a technology that decomposes complex signals into simple signals. It mainly analyzes dynamic noise signals in the frequency domain through Fourier transform. The frequency spectrum refers to the representation of a time domain signal under the frequency domain. The Fourier transform is performed on the signal, and the obtained results have amplitude and phase as the vertical axis and frequency as the horizontal axis.

3.1 Sequence Diagram

Sequence graph [13] is an interactive graph in the system dynamic model, which describes the sequence of messages passing between the various roles in performing system functions, focusing on the time sequence. The basic theory of a sequence diagram: according to the observed data, to establish the dynamic dependency relationship of the time series of the research object and the model. The model is used to evaluate the current situation of the research object and estimate the future change of the research object, and then the research object is predicted. If the statistical properties of a stochastic process remain unchanged after the time translation, i.e

$$\Phi(P_1, t) = \Phi(P_1, t+\tau) \quad (1)$$

The process is called stationary random process.

3.2 Periodogram

Periodic graph [14] refers to the intensity diagram of periodic variation

$$I(f_i) = \frac{N}{2}(a_i^2 + b_i^2) \quad (2)$$

Where N is the number of observations, a_i and b_i are Fourier coefficients, and $I(f_i)$ is the intensity of frequency f_i. The basic principle of periodogram is that the observed data are directly Fourier transformed, and then the square of the modulus is the power spectrum. The finite observation points of stationary signal $x(n)$ are taken as $x(0)$, $x(1)$, ..., $x(n\text{-}1)$. Take Fourier transform as follows [15]:

$$X_N(e^{-jw}) = \sum_{n=0}^{N-1} x(n)e^{-jwn} \quad (3)$$

In the periodic method, the N-point observation data $x_N(n)$ of the random signal $x(n)$ is regarded as the energy limited signal, Fourier transform of $x_N(n)$ is taken to obtain $x_N(w)$, and then the square of its amplitude is divided by N to estimate the true power spectrum $P(e^{jw})$ of $x(n)$

$$\tilde{P}(w) = \frac{1}{N}\left|X_N(e^{-jw})\right|^2 = \frac{1}{N}\left|\sum_{n=0}^{N-1} x(n)e^{-jwn}\right|^2 \quad (4)$$

Fourier transform is to express a certain function that satisfies certain conditions as a trigonometric function or a linear combination of their integrals. The theorem is applied to periodogram and power spectrum estimation. Discrete Fourier Transform [16]:

$$F(\omega) = [F(t)] = \int_{-\infty}^{\infty} f(t)e^{-iwt}dt \quad (5)$$

Among them, the random signal $f(t)$ is a non-periodic real function of time t. Channel capacity of periodogram is as follows.

A_1 = [51.47, 4.54, 16.8, **8.43**, **8.43**, 16.8, 4.54],

A_2 = [52.45, 12.33, 5.81, 11.12, **9.91**, **9.91**, 11.12, 5.81, 12.32],

A_3 = [52.59, 13.03, 12.25, 14.83, **0.93**, **0.93**, 14.83, 12.25, 13.03],

A_4 = [52.44, 11.49, 9.25, 9.48, **-16.86**, **-16.86**, 9.48, 9.25, 11.49],

A_5 = [52.44, 7.22, 10.65, 6.49, **8.99**, **8.99**, 6.49, 10.65, 7.22].

3.3 Density Graph

Density graph is a theoretical graphical representation of boundary objects corresponding to data values. The horizontal axis of the density graph represents the noise frequency separated by Fourier transform, and the vertical axis represents the amplitude spectral density. The Fourier transform of noise autocorrelation function is the power spectral density function [17]:

$$R(\tau) = \lim_{T\to\infty}\frac{1}{2T}\int_{-T}^{T} p(t)\cdot p(t-\tau)dt$$

$$S(w) = \int_{-\infty}^{\infty} R(\tau)e^{-jw\tau}d\tau \quad (6)$$

If the power spectrum of noise is uniform, it is called white noise. The power spectral density of a stationary random process is the Fourier transform of its autocorrelation function

$$S(\omega) = \int_{-\infty}^{+\infty} R(\tau)e^{-j\omega\tau}d\tau \quad (7)$$

From the inverse Fourier transform formula, there are

$$R(\tau) = \frac{1}{2\pi}\int_{-\infty}^{+\infty}\frac{N_0}{2}e^{j\omega\tau}d\omega \quad (8)$$

The above two formulas are collectively called the Wiener-Khinchin formula [18]. If a stationary process $\{W(t), t\geq 0\}$ has a constant power spectral density $S(\omega) = \frac{N_0}{2}, \omega = (-\infty, \infty)$, then $W(t)$ is called a white noise process. N_0 is the unilateral power spectral density, which is a constant in W/Hz. According to Wiener-Khinchin formula, the autocorrelation function of white noise process is obtained [19]

$$R(\tau) = \frac{1}{2\pi}\int_{-\infty}^{+\infty}\frac{N_0}{2}e^{j\omega\tau}d\omega = \frac{N_0}{2}\cdot\frac{1}{2\pi}\cdot 2\pi\delta(\tau) = \frac{N_0}{2}\cdot\delta(\tau) \quad (9)$$

The autocorrelation function of white noise is an impulse function located at τ=0 that is, the white noise is only correlated at $N_0/2$, but the random values at any two different times are not correlated. White noise fluctuates rapidly with time and has a wide frequency spectrum. Channel capacity of density graph is as follows.

B_1 = [103.04, 53.0, 61.87, 55.67, 55.67, 61.87, 53.01],

B_2 = [104.96, 65.08, 54.93, 53.05, 56.03, 56.03, 53.05, 54.93, 65.08],

B_3 = [105.26, 57.72, 62.33, 62.73, 60.11, 60.11, 62.73, 62.33, 57.72],

B_4 = [105.08, 64.93, 61.56, 58.49, 56.93, 56.93, 58.49, 61.56, 64.93],

B_5 = [105.03, 55.50, 48.12, 47.12, 51.93, 51.94, 47.12, 48.12, 55.50].

3.4 Welch Algorithm

The window function is a signal with finite width in time domain. The steps of window function in underwater noise signal processing: firstly, a time series is intercepted from the signal. Secondly, the virtual signal is obtained by the periodic extensive processing of the intercepted time series. Finally, the signal is processed by fast Fourier transform to get the analysis spectrum of the noise signal.

The Fourier transform (FFT) is the extended discrete signal for spectrum analysis and the analysis spectrum is the approximation of the actual spectrum. Spectrum energy leakage refers to the phenomenon that the signal spectrum is tailed and widened due to the convolution in frequency domain when the window function is used to truncate the signal in time domain. Welch algorithm is a combination of windowing and averaging.

Welch algorithm first multiplies the segmented data by the window function to add windows, and then calculates the periodogram respectively. Then, the average power spectrum is obtained

$$\tilde{P}(w)=\frac{1}{MUL}\sum_{i=1}^{L}\left|\sum_{n=0}^{M}x^{i}{}_{m}(n)e^{-jwn}\right|^{2} \quad (10)$$

Where $U=\sum_{n}w(n)$, $w(n)$ is the window function.

Figure 1 is a flowchart of welch power spectrum algorithm. Welch algorithm improved periodic graph and density graph by segmenting data, partially overlapping data and using different window functions:

Step 1: Perform sampling to obtain data x (n), and divide observation data x (n) into L segments.

Step 2: Divide the data of N points into K segments, the longer each segment overlaps (the length of overlap is different).

Step 3: Set the number of welch power spectrum FFT points and estimate the length of data in superposition.

Step 4: Multiply each segment of data by the window functions and then do DFT process.

Step 5: Calculate the power spectrum of each segment of data, and then average the results of each segment to obtain an underwater noise power spectrum estimate.

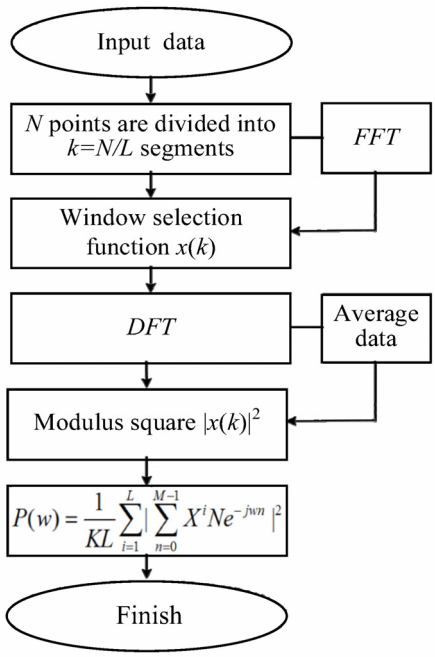

Figure 1. Welch algorithm steps

4 Spectrum Analysis of Noise

Through the noise sequence diagram, periodogram, density diagram, and combined with the noise voltage intensity, frequency and amplitude of different sites to research the noise characteristics.

4.1 Noise Sequence Diagram

According to Figure 2, the 5-day point noise sequence diagram shows that their sequences don't fluctuate randomly near a constant and the fluctuation range is unbounded. Therefore, they aren't stationary sequences. At the same time, they reflect the change of sound pressure at each point in 5 days over a period of time.

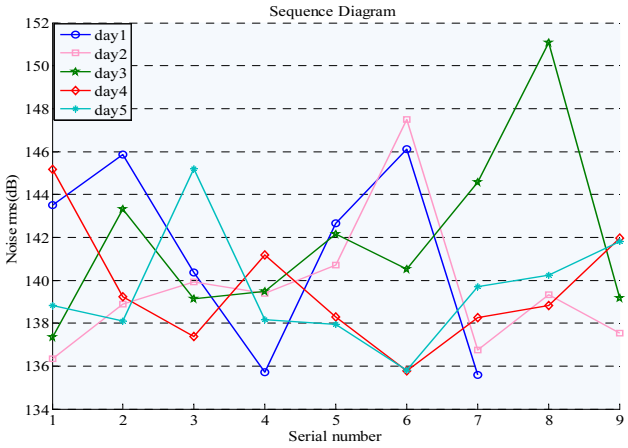

Figure 2. Noise sequence diagram of each point

4.2 Periodogram of Noise

The sample frequency is F_s=50, for the 5-day test, the number of sample sites are 7, 9, 9, 9, and 9. Given

the noise signal time series x_i=sin(2πf_1n)+sin(2πf_2n)+C_i, where C_i is the 5-day noise value obtained from the Qiongzhou Strait test in China, i=1, 2, 3, 4, 5, white noise signal the frequency f_1=0.2, f_2=0.5, n is the sample interval, and the value ranges from 0 to 8.

Figure 3 is a periodogram of noise, showing the power spectrum estimation of underwater noise for 5 days, and the periodogram can reduce random fluctuations. As shown in Figure 3, low frequency variation is a characteristic of the smooth sequence, which mainly describes the relationship between noise channel capacity and frequency. Among them, the horizontal axis represents the sample noise frequency, the vertical axis represents the noise power spectrum, and the variation of the noise channel capacity uniformly distributed on the frequency represents the white noise. Figure 3 shows that on the first day, in the range of 0 Hz to 7.14 Hz, the noise channel capacity dropped rapidly from 51.47 dB to 4.54 dB as the frequency increased, indicating that its energy distribution was rapidly decreasing. From the range of 7.14 Hz - 21.43 Hz and 28.57 Hz - 42.86 Hz, the capacity of noise channel increased by the rising of its frequency, which indicates that its energy distribution is rising. In 21.43 Hz - 28.57 Hz, the noise channel capacity shows a steady trend. According to the principle of acoustics, all kinds of sound sources measured at a certain point act on the superposition value of the energy at that point, which is more effective in designing filters and selecting the types and parameters of power filter capacitors. In the 0 Hz - 5.56 Hz, the noise channel capacity increases by the frequency, and it decreases rapidly in the 2nd to 5th days. In 5.56 Hz - 16.67 Hz, 16.67 Hz - 22.22 Hz and 27.78 Hz - 38.89 Hz, the noise channel capacity increases with the frequency, it increases slowly on the 5th day and decreases slowly on the 2nd to 4th days. In 22.22 Hz - 27.78 Hz, the noise channel capacity shows a steady trend. The degree of influence of noise sources on noise is changing every day, and the noise channel capacity shows a single direction change. The negative value of the noise channel capacity indicates that the propagation direction of the signal is reversed. In order to calculate the noise channel capacity, convert these 5-day frequencies: f_1 = [0, 7.14, 14.29, 21.43, 28.57, 35.71, 42.86], q_1, u_1, w_1, z_1 = [0, 5.56, 11.11, 16.67, 22.22, 27.78, 33.33, 38.89, 44.44]. Table 2 is the time-domain resolutions of the 5-day signal plus noise.

4.3 Noise Density Diagram

For the 5-day test, a noise signal time series x_i=sin(2π×0.2×n)+sin(2π×0.5×n)+C_i is given, where C_i is the 5-day noise value obtained from the Qiongzhou strait test in China, signal frequency f_1=0.2, f_2=0.5, n=[0, 0.13, 0.25, 0.38, 0.50, 0.63, 0.75, 0.88, 1], i=1, 2, 3, 4, 5. Channel capacity y_j=10log10 (P (index+2)), Five different functions are constructed for the channel capacity, where j=1, 2, 3, 4, 5, bandwidth is 10, signal-to-noise ratio is index, P is an array name, P (index+2) is an array element. The log10 () is the log function, and the log 10(P (index+2)) is the log P (index+2), multiplied by the bandwidth of 10.

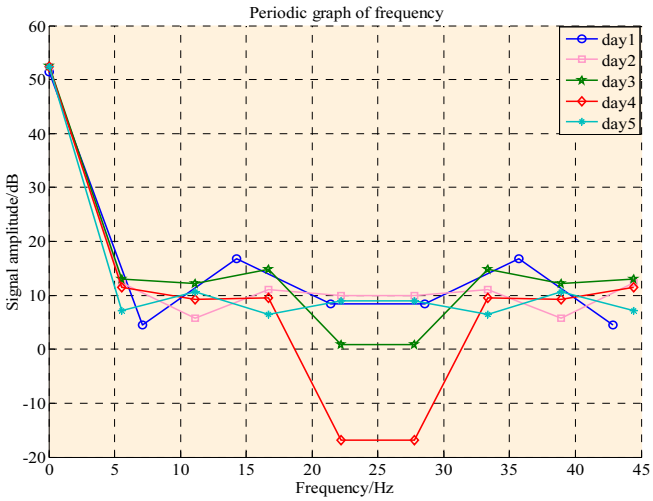

Figure 3. Noise period diagram of each point

Table 2. Time-domain resolutions of signal plus noise

x_1	x_2	x_3	x_4	x_5
143.59	136.42	137.42	145.26	138.9
145.94	138.98	143.38	139.31	138.2
140.46	140.01	139.22	137.47	145.28
135.81	139.48	139.58	141.27	138.26
142.73	140.81	142.23	138.38	138.03
146.21	147.57	140.62	135.88	135.9
135.67	136.83	144.67	138.34	139.78
-	139.43	151.17	138.92	140.32
-	137.61	139.27	142.04	141.9

Figure 4 shows the density map of underwater noise, which can reflect the noise intensity at different locations and times. The value obtained by the autocorrelation function of the sequence is symmetric, which means that the time sequence of the density graph is non-stationary, so the sequence cannot be used to predict the noisy characteristics. The reason generating the underwater noise is what we cann't explain, such as climate. Therefore, it is difficult to explain the changes of the underwater noise by models because of the corresponding quantitative data and suitable regression model. The noise spectral density means that the closer the density, the more severe the noise. Since the total energy contained by the time waveform is finite, it is equal to the sum of the energy of all components, and the amplitude of each component must be infinitesimal. Therefore, we divide the spectrum into many narrow slices, and the amplitude is proportional to the area of the narrow slice. According to the amplitude spectrum density, we can use the graphical method decomposing the spectrum, as is shown in Figure 4. Figure 4 shows that the noise at each point in 5 days is not a sequence of white noise, but colored noise. Between 0 Hz and 0.22 Hz, the spectral density of the 5-day site showed a rapid

downward trend with its frequency. Between 0.22 Hz and 0.33 Hz, the spectral density of the site on the first and third days showed a slowly upward trend with its frequency. The spectral density of the sites on the 2nd, 4th and 5th days showed a slowly downward trend with its frequency. In the range of 0.33 Hz -0.44 Hz, the spectral density of the third day increased slowly with its frequency. The spectral density of the 1st, 2nd, 4th and 5th day decreased slowly with its frequency. By analogy, it can be judged that the general density of the site varies with frequency in 0.44 Hz - 0.56 Hz, 0.67 Hz - 0.78 Hz, 0.78 Hz - 0.89 Hz, 0.78 Hz - 0.89 Hz, and 0.89 Hz - 1 Hz.

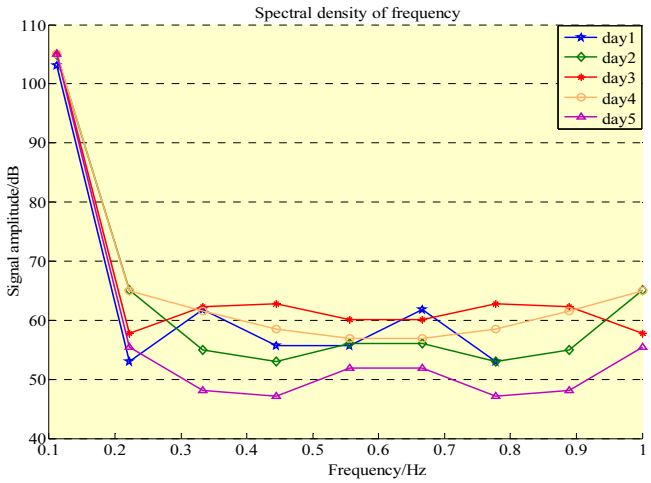

Figure 4. Noise density graph

5 Welch Algorithm

Due to the poor performance of estimating the underwater noise for the spectrum in spectrum analysis which contained by the sequence diagram, period diagram, and density diagram. Therefore, in order to improve the performance of spectrum estimation, the welch algorithm based on windowed the estimated value of the autocorrelation function and makes improvements (Table 3). The period diagram and density graph directly estimate the power spectrum. When the length of the data is too long, the power spectrum estimation curve fluctuates more and more. If the length is too short, the resolution of the spectrum is poor. Welch algorithm's segmentation and windowing of the stack length solves these two shortcomings and makes the power spectrum estimation more accurate. In order to reduce the spectrum energy leakage error and effectively satisfy the periodic requirements of Fourier processing, welch algorithm analyzes the underwater noise characteristics through four different window functions: the windows of rectangular, hamming, blackman and hanning (as shown in Figure 5).

The sample frequency is Fs=50, underwater noise signal x_i=2sin(2πn·Fs)+2cos(2πn·Fs)+C_i, where C_i is the 5-day noise value obtained from the Qiongzhou Strait test in China, sampling interval n=[0, 0.13, 0.25, 0.38, 0.5, 0.63, 0.75, 0.88, 1], i=1, 2, 3, 4, 5. Sampling number nfft=7, 9.

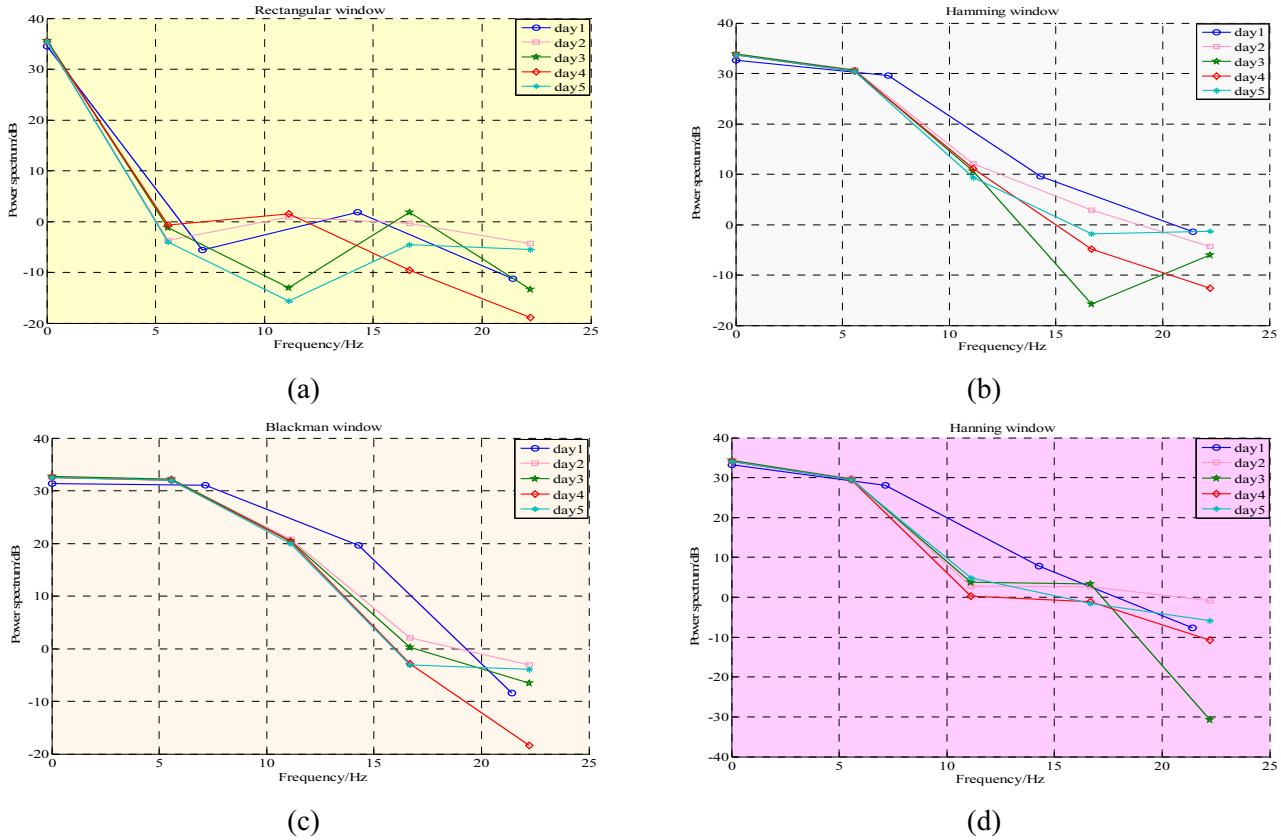

Figure 5. Power spectrum estimation of welch algorithm

Table 3. Comparison of periodogram method and superposition welch algorithm

Periodogram					Welch algorithm				
Day1	Day2	Day3	Day4	Day5	Day1	Day2	Day3	Day4	Day5
51.47	52.45	52.59	52.44	52.44	31.33	32.69	32.68	32.5	32.51
4.54	12.33	13.03	11.49	7.22	31	32.24	32.17	32.01	31.97
16.8	5.81	12.25	9.25	10.65	19.59	20.78	20.5	20.37	19.97
8.43	11.12	14.83	9.48	6.49	-8.45	2.01	0.26	-2.9	-3.14
8.43	**9.91**	**0.93**	**-16.86**	**8.99**		-3.09	-6.53	-18.42	-3.98
16.8	**9.91**	**0.93**	**-16.86**	**8.99**					
4.54	11.12	14.83	9.48	6.49					
	5.81	12.25	9.25	10.65					
	12.32	13.03	11.49	7.22					

Through the four windows, the noise channel capacity of 5 days is obtained as follows: {[34.49, -5.58, 1.8, -11.3], [35.46, -3.69, 0.85, -0.33, -4.38], [35.6, -1.26, -13, 1.79, -13.37], [35.46, -0.68, 1.48, -9.57, -18.88] and [35.46, -4.034, -15.63, -4.55, -5.53]}, {[32.6, 29.55, 9.58, -1.43], [33.83, 30.75, 12.14, 2.85, -4.31], [33.87, 30.63, 10.59, -15.73, -6.03], [33.68, 30.46, 11.11, -4.86, -12.65] and [33.7, 30.43, 9.33, -1.80, -1.33]}, {[31.33, 31, 17.59, -8.45], [32.69, 32.24, 20.78, 2.01, -3.09], [32.68, 32.17, 20.5, 0.26, -6.53], [32.5, 32.01, 20.37, -2.9, -18.42] and [32.51, 31.97, 19.97, -3.14, -3.98]}, {[33.26, 28.01, 7.86, -7.68], [34.21, 29.81, 2.85, 2.66, -0.86], [34.28, 29.65, 3.76, 3.39, -30.67], [34.08, 29.5, 0.3, -1.13, -10.78] and [34.11, 29.47, 4.92, -1.51, -5.82]}.

We choose the appropriate window function $w(n)$, and directly add it before the periodogram calculation. Appropriate non-rectangular window to process the signal can reduce the spectral leakage and increase the width of the frequency peak, thereby improving the spectral resolution. In the segmentation, overlap among the segments, which will reduce the variance. Welch algorithm uses signal overlapping segmentation, the windowing function and FFT algorithm to calculate the self-power spectrum estimation of a signal sequence. By comparing the periodogram method with the welch algorithm with the addition of the Blackman window function, it is obvious that the resolution of the latter is better than the former, and the spectrum estimation is more accurate.

Using the welch algorithm to establish the power spectrum model to estimate the underwater noise power spectrum model under different voltage intensities for the data. Figure 5 shows that the four window functions that the power spectrum under different voltage intensities show a downward trend as the frequency increases. In the rectangular window power spectrum estimation, the first day showed a downward tendency at 0 Hz - 7.14 Hz and 14.29 Hz - 21.43 Hz and an upward tendency from 7.14 Hz to 14.29 Hz. The 2nd, 3rd, 4th and 5th day showed a downward trend from 0 Hz to 5.56 Hz. In 5.56 Hz - 11.11 Hz, the 2nd and 4th days showed an upward trend. The 3rd and 5th days showed a downward trend. In 11.11 Hz - 16.67 Hz, the 3rd and 5th days showed an upward trend. The 2nd and 4th days showed a downward trend. In 16.67 Hz - 22.22 Hz, it showed a downward trend for 5 days. In the Hamming window spectrum estimation, the first day showed a downward trend. On the 2nd, 3rd, 4th and 5th day, there was a slow downward trend from 0 Hz - 5.56 Hz. In 5.56 Hz - 16.67 Hz, the 2nd, 3rd, 4th and 5th days showed a downward tendency. Between 16.67 Hz - 22.22 Hz, the 2nd and 4th days showed a downward tendency. The 3rd and 5th days showed an upward tendency. In the estimation of the blackman window power spectrum, between 0 Hz and 7.14 Hz, the first day tends to be stable. 0 Hz - 7.14 Hz, 14.29 Hz - 21.43 Hz and 7.14 Hz - 14.29 Hz showed a downward trend. In 0 Hz - 16.67 Hz, the 2nd, 3rd, 4th and 5th day showed a downward trend. Between 16.67 Hz and 22.22 Hz, the 2nd, 3rd, and 4th days showed a downward trend, and the 5th day showed an upward trend. In the hanning window power spectrum estimation, 0 Hz - 7.14 Hz, 14.29 Hz - 21.43Hz, 7.14 Hz - 14.29Hz, the first day showed a downward trend. From 0 Hz - 11.11 HZ, the 2nd, 3rd, 4th and 5th day showed a slow downward trend. Between 11.11 Hz - 16.67 Hz, the 2nd and 3rd days showed a slow upward trend. The 4th and 5th days showed a slow downward trend. Between 16.67 Hz and 22.22 Hz, the 2nd, 3rd, 4th and 5th day all showed a downward trend.

Figure 5(*a*) shows the welch power spectrum algorithm with rectangular window, which mainly makes the main lobe of the power spectrum of underwater noise more concentrated, the frequency identification accuracy is the highest, the amplitude identification accuracy is the lowest, but the side lobes are higher, and there are negative side lobes. Lobe, resulting in high-frequency interference and leakage in the transformation, and even negative spectrum phenomenon. Figure 5(b) represents welch power spectrum algorithm with the Hamming window. It is a cosine window with hanning window, but the weighting coefficient is different, which makes the side lobes smaller. However, the attenuation speed of the side lobe is slower than that of hanning window. Figure 5(c) represents the welch power spectrum algorithm with Blackman window, the second-order raised cosine window, the main lobe is wide, the side lobe is relatively low, but the equivalent noise

bandwidth is larger than hanning window, and the fluctuation is smaller. The accuracy of frequency recognition is the lowest, but the amplitude recognition accuracy is the highest, with better selectivity. Figure 5(d) represents welch power spectrum algorithm with hanning window. The main lobe is widened and reduced, while the side lobes are significantly reduced. From the viewpoint of reducing leakage, hanning window is better than rectangular window. But the main lobe of the hanning window is widened, which is equivalent to widening the analysis bandwidth and decreasing the frequency resolution. Compared with the rectangular window, leakage and fluctuation are reduced, and the selectivity is also improved. Using four window functions can make the prediction of underwater noise characteristics more accurate, avoiding the advantages and disadvantages of each window function. From the perspective of the four window functions, the Blackman window is the best choice because its second-order raised cosine window has a wide main lobe and lower side lobes, but the equivalent noise bandwidth is a bit larger than hanning window, and the fluctuation is smaller. Frequency recognition accuracy is the lowest, but amplitude recognition accuracy is the highest, so it is the best.

6 Conclusion

We use periodogram, sequence diagram and density diagram and improved welch algorithm to analyze the underwater noise data at different locations in 5 days through windowing function. The periodogram method estimates the frequency by searching the power spectrum peaks of the signal without calculating the autocorrelation function, which is simple to achieve and has stable performance. But its performance is affected by noise frequency resolution and random errors. Segmentation process of welch algorithm reduces the resolution of the noise frequency and the random error, which has a higher algorithm complexity than the periodogram method. In addition, the stack length of welch algorithm is improved. The stack length of each segment is different, which makes the power spectrum estimate more accuracy than the previous average stack length. At the same time, four windowing functions are used to compare with the periodogram method. When the total amount of data is larger than 10, the simulation effect obtained by welch algorithm is more accurate than the result of the periodogram method.

Acknowledgements

This work is supported by National Natural Science Foundation of China (Grant No. 61962017), Natural Science Foundation of Hainan Province (No. 2019RC085, 2019RC088, and 119MS002), and Fundamental Research Funds for the Central Universities (2020ZYGXZR042). It grants from State Key Laboratory of Marine Resource Utilization in South China Sea and Key Laboratory of Big Data and Smart Services of Hainan Province.

References

[1] X. Luo, Z. Shen, A Space-frequency Joint Detection and Tracking Method for Line-spectrum Components of Underwater Acoustic Signals, *Applied Acoustics*, Vol. 172, Article No. 107609, January, 2021.

[2] N. D. Merchant, T. R. Barton, P. M. Thompson, E. Pirotta, D. T. Dakin, J. Dorocicz, Spectral Probability Density as a Tool for Ambient Noise Analysis, *Journal of the Acoustical Society of America*, Vol. 133, No. 4, pp. 262-267, April, 2013.

[3] Q. Qi, H. Chen, Z. Yan, L. Li, G. Zhu, Holographic Reconstruction Research on the Radiated Acoustic Field of the Underwater Vehicle, *Oceans*, Marseille, France, 2019, pp. 1-5.

[4] C. Meng, D. Song, F. Cao, X. Zhang, J. Han, J. Bai, Statistical Characteristic of Spectrum for Ambient Noise at High Frequencies in Shallow Water, *IEEE International Conference on Signal Processing, Communications and Computing*, Xiamen, China, 2017, pp. 1-4.

[5] J. M. Hovem, R. Vagsholm, H. Sorheim, B. Haukebo, Measurements and Analysis of Underwater Acoustic Noise of Fishing Vessels, *Oceans Conference*, Genoa, Italy, 2015, pp. 1-6.

[6] J. Liu, Research on the Characteristics Analysis Method of Ship Underwater Transient Noise, *China Science and Technology Information*, No. 7, pp. 67-70, April, 2014.

[7] Z. Huang, *Frequency Estimation of Line Spectrum Signal*, Master Thesis, Southeast University, Jiangsu, China, 2014.

[8] A. Z. Shaameri, Y. Y. Al-Aboosi, N. H. H. Khamis, Underwater Acoustic Noise Characteristics of Shallow Water in Tropical Seas, *International Conference on Computer & Communication Engineering*, Kuala Lumpur, Malaysia, 2014, pp. 80-83.

[9] S. Yan, C. Kang, Z. Xia, K. Li, Classification and Recognition of Ship Radiated Noise Based on Deep Auto-encoding Networks, *Ship Science and Technology*, Vol. 41, No. 2, pp. 124-130, February, 2019.

[10] X. Cui, K. He, K. Lei, W. Shi, H. Wang, Simulation of Propagation Properties of Underwater Narrow Pulse and UWB Signal, *Computer Measurement and Control*, Vol. 23, No. 1, pp. 218-220, January, 2015.

[11] T. Ju, T. Zhang, Z. Wang, Y. Xie, C. Zheng, K. Wang, D. Wang, Characteristics of Riprapping Underwater Noise and Its Possible Impacts on the Yangtze Finless Porpoise, *Technical Acoustics*, Vol. 36, No. 6, pp. 580-588, December, 2017.

[12] Z. Yan, Q. Zhang, Radiated Noise Line Spectrum Extraction of Underwater Target Based on Welch Power Spectrum Estimation and Median Filtering, *Computer Engineering and Applications*, Vol. 52, No. S2, pp. 230-233, October, 2017.

[13] D. Yi, Y. Wang, *Applied Time Series Analysis*, China Renmin

University Press, 2019. ISBN：9787300270272

[14] Y. Zhang, *Sparse Signal Processing and Its Applications in Underwater Acoustics*, Harbin Institute of Technology Press, 2020. ISBN：9787560377483

[15] Q. Deng, *Research on the Mechanism and Control of the Underwater Acoustic Radiation from Offshore Pile Driving*, PhD Thesis, Shanghai Jiao Tong University, Shanghai, China, 2016.

[16] H. Boche, U. J. Mönich, Turing Computability of Fourier Transforms of Bandlimited and Discrete Signals, *IEEE Transactions on Signal Processing*, Vol. 68, pp. 532-547, January, 2020.

[17] F. Ni, Y. Zhou, H. Liu, Microphone Array Noise Elimination Method Using Signal Power Spectral Density, *Journal of Signal Processing*, Vol. 36, No. 3, pp. 373-381, March, 2020.

[18] X. Qi, C. Chen, Y. Qu, X. Zhang, Y. Chen, B. Wang, L. Liang, P. Jia, L. Qin, Y. Ning, L. Wang, Complete Frequency Domain Analysis for Linewidth of Narrow Linewidth Lasers, *Spectroscopy and Spectral Analysis*, Vol. 39, No. 8, pp. 2354-2359, August, 2019.

[19] X. Xing, G. Zhu, Window Function Selection and Algorithm Analysis in Welch Power Spectrum Estimation, *Computer Era*, No. 2, pp. 1-4, February, 2018.

Biographies

Hui Zhou received Ph.D. degree from University of Chinese Academy of Science. Dr. Zhou has been an associate professor of Hainan University since 2011. Dr. Zhou is in charge of several research projects including the National Natural Science Funds projects. His research interests include data visualization, marine communication, writing robot. Email: zhouhui@hainanu.edu.cn.

Biyuan Yao is currently pursuing her Ph.D. degree in School of Computer Science and Engineering (CSE), South China University of Technology (SCUT), China. Her research interests include marine communication, and graph theory with applications. Email: yaobiyuanyy@163.com.

Kun Ye is a master student of in School of Science, Hainan University, China. His research interests include graph theory with applications. Email: yekun_eric@163.com.

Guiqing Li is a professor of the School of CSE in SCUT. His research interests include computer graphics, dynamic geometry processing, and image and video processing. Email: ligq@scut.edu.cn.

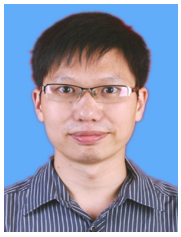

Jin Guo received Ph.D. degree from Shanghai Jiaotong University. Dr. Guo has been an associate professor of Hainan University since 2018. Dr. Guo is in charge of the National Natural Science Funds projects 3 times. His research interests include combinatorial commutative algebra, zero-divisor graphs. Email: guojinecho@163.com.